Quark matter under strong magnetic fields in chiral models

Aziz Rabhi[1,2,*] and Constança Providência[1,†]

[1]*Centro de Física Computacional, Department of Physics, University of Coimbra, P-3004-516 Coimbra, Portugal*

[2]*Laboratoire de Physique de la Matière Condensée, Faculté des Sciences de Tunis, Campus Universitaire, Le Belvédère-1060, Tunisia*

(Received 9 February 2011; revised manuscript received 5 April 2011; published 3 May 2011)

The chiral model is used to describe quark matter under strong magnetic fields and is compared to other models, the MIT bag model and the two-flavor Nambu-Jona-Lasinio model. The effect of vacuum corrections due to the magnetic field is discussed. It is shown that if the magnetic-field vacuum corrections are not taken into account explicitly, the parameters of the models should be fitted to low-density meson properties in the presence of the magnetic field.

DOI: 10.1103/PhysRevC.83.055801 PACS number(s): 26.60.−c, 12.39.−x, 21.65.Qr, 24.10.Jv

I. INTRODUCTION

Magnetars, neutron stars with very strong magnetic fields of the order of 10^{14}–10^{15} G at the surface, are sources of very energetic electromagnetic radiation, mainly gamma and x rays [1–3]. Presently, approximately 21 of these objects have been detected, most of them as soft gamma repeaters (SGRs) and anomalous x-ray pulsars (AXPs) [4].

It has been argued [5] that *strange quark matter* (SQM), i.e., quark matter with strangeness per baryon of the order of unity, may be the true ground state of hadronic matter. This could imply that compact stars are mainly quark stars (see also Ref. [6]). Magnetars as compact quark stars have been first investigated in Ref. [7], where the MIT bag model [8] was applied to obtain the equation of state (EOS) of stellar quark matter under magnetic fields as strong as 10^{18} G. The EOS for magnetized quark stars described within the MIT bag model and taking into account the anomalous magnetic moment of quarks (AMM) was studied in Ref. [9]. The su(2) version of the Nambu-Jona-Lasinio model (NJL) [10], an effective model which includes the chiral symmetry, was applied to study the stability of quark matter under very strong magnetic fields in Ref. [11]. The same model and its su(3) extension were used to describe quark stars with very large magnetic fields in Refs. [12] and [13]. In these papers, the phenomenon of magnetic catalysis within the NJL models has been discussed. Magnetic catalysis is one of the most important effects of the magnetic field in quark models with chiral symmetry and corresponds to the enhancement of the chiral symmetry breaking in the magnetic field [14]. Another nontrivial effect of the magnetic field is the possibility that strong magnetic fields can turn a crossover into a first-order quantum chromodynamical (QCD) transition [15].

A different quark model with chiral symmetry, the chiral model of pions and quarks or nucleons [16–18], also known as the linear sigma model, was applied to study the high-density npeμ matter with π^0 condensation [19]. In the present work we will use the same model to describe both symmetric quark matter and stellar quark matter under strong magnetic fields. No pion condensation will be considered. The results will be compared with the MIT and NJL models. In particular, we will investigate the inclusion of vacuum corrections due to the strong magnetic field.

The linear sigma model coupled to quarks and the Polyakov loop has been recently used to study the phase diagram of hot QCD in a strong external magnetic field [20]. There it was shown that a strong magnetic field could give rise to a splitting of the deconfinement and chiral transitions if the B-dependent vacuum corrections were included. These results agree well with the diagram coming from the NJL model [21], where the vacuum corrections are present authomatically, and with the results of the lattice calculations [22].

The MIT bag model describes quarks as a free gas of quarks already in a chiral restored state. The bag pressure provides the confinement and is just a parameter which can be fixed from the nucleon sector. The problem of chiral symmetry restoration is beyond the scope of this model. Both NJL and the chiral model are described by chiral symmetric Lagrangian densities and a vacuum state with spontaneously broken chiral symmetry. In the chiral model, the chiral condensate plays the role of the bag pressure and its value in the vacuum is fixed from the pion decay constant, which is well known, and the sigma mass. The connection between the MIT bag model and the chiral model has been discussed in Ref. [23]. In the NJL model the model parameters are fixed by fitting the pion decay constant and the quark condensate.

In Sec. II we make a brief review of the three models and their corresponding EOS under the effect of a magnetic field and discuss how the model parameters are fixed for a finite magnetic field. Results are discussed in Sec. III and conclusions are drawn in Sec. IV.

II. QUARK MODELS

In the present section we give a brief review of the quark models, including the effect of a strong magnetic field used in this study: the chiral sigma model, the su(2) NJL model, and the MIT bag model.

A. Chiral sigma model

We consider the chiral sigma model for quarks interacting with an external magnetic field. The chiral symmetric

*rabhi@teor.fis.uc.pt
†cp@teor.fis.uc.pt

Lagrangian density reads [16,18]

$$\mathcal{L} = \bar{\psi}_f(i\gamma_\mu\partial^\mu - \hat{q}\gamma_\mu A^\mu - g(\sigma + i\gamma_5\vec{\tau}\cdot\vec{\pi}))\psi_f + \tfrac{1}{2}\partial_\mu\sigma\partial^\mu\sigma + \tfrac{1}{2}\partial_\mu\pi^0\partial^\mu\pi^0 + D_\mu\pi^+D^\mu\pi^- - U(\sigma,\vec{\pi}) - \tfrac{1}{4}F^{\mu\nu}F_{\mu\nu}, \quad (1)$$

where ψ_f is the quark field, σ and π^0, $\pi^\pm = (\pi^1 \pm i\pi^2)/\sqrt{2}$ are the meson fields, $D^\mu = \partial^\mu + ieA^\mu$, g is the quark-meson coupling constant, $\hat{q} = (\frac{1}{3} + \tau_3)e/2$, and $A^\mu = (0, 0, Bx, 0)$ refers to an external magnetic field along the z-axis.

The potential functional U is a "Mexican hat" potential, which leads to spontaneous chiral symmetry breaking and is included to reproduce the vacuum expectation value of the sigma field. For exact chiral symmetry ($m_\pi = 0$), the potential is

$$U(\sigma,\vec{\pi}) = \frac{\lambda^2}{4}\left(\sigma^2 + \vec{\pi}^2 - f_\pi^2\right)^2, \quad (2)$$

where $\lambda^2 = \frac{m_\sigma^2}{2f_\pi^2}$, and m_σ is the mass of the σ meson. The vacuum expectation value of the field σ is $\langle\sigma\rangle = f_\pi$, where $f_\pi = 93$ MeV is the pion decay constant in the absence of a magnetic field. In the normal phase with no pion condensation, the energy density is given by

$$\mathcal{E} = \sum_{f=u,d}\frac{N_c|q_f|B}{2\pi^2}\sum_{\nu=0}^{\nu_{f,\max}}\alpha_\nu \times \int_0^{p_{F,f\nu}} dp_z\sqrt{p_z^2 + m^2 + 2\nu|q_f|B} + U(\sigma,0), \quad (3)$$

where $m = g\sigma$, and $\nu = n + \frac{1}{2} - \mathrm{sgn}(q)\frac{s}{2} = 0, 1, 2, \ldots$ enumerates the Landau levels (LLs) of the fermions with electric charge q, the factor $\alpha_\nu = 1$, (2) for $\nu = 0$ ($\nu \geqslant 1$) takes care of singly degenerate zeroth LL and doubly degenerate LL levels with $\nu \geqslant 1$, and the Fermi momentum of LL ν is $p_{F,f\nu} = \sqrt{\mu_f^2 - M_f^2(\nu, B)}$. The coefficient $N_c = 3$ stands for the color degeneracy. We use $m_\sigma = 1200$ MeV.

The energy minimization for each baryon density, with respect to the σ field, gives the so-called gap equation

$$\sum_{f=u,d}\frac{N_c|q_f|B}{2\pi^2}\sum_{\nu}^{\nu_{f,\max}}\alpha_\nu \times \int_0^{p_{F,f\nu}}\frac{dp_z}{\sqrt{p_z^2 + m^2 + 2\nu|q_f|B}} + \frac{\partial U}{\partial\sigma} = 0. \quad (4)$$

The mass in the vacuum is $m_0 = gf_\pi$. In the presence of a strong magnetic field the vacuum properties are affected and a quark vacuum correction should be included [12,20]. This correction was not considered in Ref. [19]. Since the magnetic fields discussed were below 6×10^{18} G, we do not expect a large effect coming from this term. We will take into account this correction in two different ways: (a) We will redefine the constant f_π and suppose all vacuum effects are described by the "Mexican hat," including the magnetic-field contribution; and (b) we consider that the "Mexican hat" potential does not include the magnetic-field vacuum contribution, and we will add this contribution explicitly as an extra term to (2) just as it was done in Ref. [20].

B. The MIT bag model

In the presence of a strong magnetic field, the energy density and quark density within the MIT bag model are given by [24]

$$\varepsilon_m = \sum_{f=u,d}\frac{N_c|q_f|B}{4\pi^2}\sum_{\nu=0}^{\nu_{f,\max}}\alpha_\nu \times\left[\mu_f\, p_{F,f\nu} + M_f^2(\nu, B)\ln\left|\frac{\mu_f + p_{F,f\nu}}{M_f(\nu, B)}\right|\right] + \mathrm{Bag}, \quad (5)$$

$$\rho_q = \sum_{f=u,d}\frac{N_c|q_f|B}{2\pi^2}\sum_{\nu=0}^{\nu_{f,\max}}\alpha_\nu p_{F,f\nu}, \quad (6)$$

where $M_f(\nu, B) = \sqrt{m_f^2 + 2\nu|q_f|B}$ and ν runs over the allowed LL, m_q is the quark mass, and Bag represents the bag pressure. We only consider flavors u and d.

C. The su(2) NJL model

We consider the two-flavor NJL model defined by the following Lagrangian density [12,13]:

$$\mathcal{L} = \mathcal{L}_f - \tfrac{1}{4}F_{\mu\nu}F^{\mu\nu}, \quad (7)$$

where the quark sector is described by the Nambu-Jona-Lasinio model,

$$\mathcal{L}_f = \bar{\psi}_f[\gamma_\mu(i\partial^\mu - \hat{q}A^\mu) - m_c]\psi_f + G[(\bar{\psi}_f\psi_f)^2 + (\bar{\psi}_f i\gamma_5\vec{\tau}\psi_f)^2], \quad (8)$$

$m_c = m_u \simeq m_d$ are the quark current masses; A_μ and $F_{\mu\nu} = \partial_\mu A_\nu - \partial_\nu A_\mu$ are used to account for the external magnetic field. Since we are interested in a static and constant magnetic field in the z direction, $A_\mu = \delta_{\mu 2}x_1 B$.

The energy density is given by

$$\mathcal{E}(\mu_f, B) = -P^N + \sum_f \mu_f\rho_f, \quad (9)$$

where μ_f is the chemical potential of flavor f and the pressure is $P^N = P(\mu_f)|_{M(\mu_f)} - P(0)|_{M(0)}$ with

$$P = \theta_u + \theta_d - G(\phi_u + \phi_d)^2. \quad (10)$$

For a given flavor, the θ_f term is given by

$$\theta_f = -\frac{i}{2}\mathrm{tr}\int\frac{d^4p}{(2\pi)^4}\ln(-p^2 + M^2) \quad (11)$$

and the condensate $\phi_f = \langle\bar{\psi}_f\psi_f\rangle$, so that [12,13]

$$P = (P^{\mathrm{vac}} + P^{\mathrm{mag}} + P^{\mathrm{med}}), \quad (12)$$

where the vacuum contribution reads

$$P^{\mathrm{vac}} = -\frac{N_c N_f}{8\pi^2}\left[M^4\ln\left(\frac{\Lambda + \epsilon_\Lambda}{M}\right) - \epsilon_\Lambda\Lambda\left(\Lambda^2 + \epsilon_\Lambda^2\right)\right], \quad (13)$$

with $\epsilon_\Lambda = \sqrt{\Lambda^2 + M^2}$, Λ representing a noncovariant ultraviolet cutoff; the finite magnetic contribution is

$$P^{\rm mag} = \sum_{f=u,d} \frac{N_c(|q_f|B)^2}{2\pi^2} \times \left[\zeta'(-1, x_f) - \frac{1}{2}(x_f^2 - x_f)\ln x_f + \frac{x_f^2}{4}\right], \quad (14)$$

with $x_f = M^2/(2|q_f|B)$ and $\zeta'(-1, x_f) = d\zeta(z, x_f)/dz|_{z=-1}$, where $\zeta(z, x_f)$ is the Riemann-Hurwitz zeta function, and the medium contribution can be written as

$$P_M^{\rm med} = \sum_{f=u,d} \frac{|q_f|BN_c}{4\pi^2} \sum_{\nu=0}^{\nu_{f,\max}} \alpha_\nu \left[\mu_f p_{F,f\nu} - M_f(\nu, B)^2 \times \ln\left|\frac{\mu_f + p_{F,f\nu}}{M_f(\nu, B)}\right|\right] - G(\phi_u + \phi_d)^2, \quad (15)$$

where $M_f(\nu, B) = \sqrt{M^2 + 2|q_f|B\nu}$ and $p_{F,f\nu} = \sqrt{\mu_f^2 - M_f(\nu, B)^2}$. The upper LL (or the nearest integer) is defined by

$$\nu_{f,\max} = \frac{\mu_f^2 - M^2}{2|q_f|B} = \frac{p_{f,F}^2}{2|q_f|B}. \quad (16)$$

The effective quark masses can be obtained self-consistently from

$$M = m_c - 2G(\phi_u + \phi_d), \quad (17)$$

where the condensates ϕ_f are given by

$$\phi_f = \left(\phi_f^{\rm vac} + \phi_f^{\rm mag} + \phi_f^{\rm med}\right)_M, \quad (18)$$

with

$$\phi_f^{\rm vac} = -\frac{MN_c}{2\pi^2}\left[\Lambda\epsilon_\Lambda - M^2\ln\left(\frac{\Lambda + \epsilon_\Lambda}{M}\right)\right], \quad (19)$$

$$\phi_f^{\rm mag} = -\frac{M|q_f|BN_c}{2\pi^2}\left[\ln\Gamma(x_f) - \frac{1}{2}\ln(2\pi) + x_f - \frac{1}{2}(2x_f - 1)\ln(x_f)\right], \quad (20)$$

and

$$\phi_f^{\rm med} = \frac{M|q_f|BN_c}{2\pi^2}\sum_{\nu=0}^{\nu_{f,\max}} \alpha_\nu \ln\left(\frac{\mu_f + p_{F,f\nu}}{M_f(\nu, B)}\right). \quad (21)$$

The density, ρ_f, corresponding to each different flavor, is given by Eq. (6).

For the su(2) NJL model we use the same parametrization as given in Ref. [25]: $\Lambda = 587.9$ MeV, $m_c = 5.6$ MeV, $m_e = 0.511$ MeV, $m_\mu = 105.66$ MeV, and $G\Lambda^2 = 2.44$, which gives a quark vacuum mass equal to 400 MeV in the absence of a magnetic field.

D. Fixing the model parameters at finite B

In order to compare the MIT bag model with the other two models we chose Bag $= 0.9$ fm$^{-4} = 177.3$ MeV/fm^3, which is in between the values we get for the chiral model and the NJL model in the chiral symmetric density region. We note that in MFT, when the chiral symmetry is restored, i.e., ($\langle\sigma\rangle = 0$ and $\langle\vec{\pi}\rangle = 0$), the potential functional reduces to a constant energy density equal to $\frac{\lambda^2}{4}f_\pi^4$, and the constituent quark mass vanishes, leaving free massless quarks. The chiral Lagrangian, in the region where the chiral symmetry is restored, can be identified by a MIT bag quark model with a bag pressure Bag $= \frac{\lambda^2}{4}f_\pi^4$.

In order to be able to establish a comparison between the chiral model and the NJL model, we include, in the chiral model, vacuum corrections due to the magnetic field in two different ways: (a) By renormalizing the pion constant f_π' constant so that the vacuum quark mass $m_0 = g\,f_\pi'$ in the chiral model coincides with the one obtained with the NJL model. We will call this model the chiral model I; and (b) by including in the potential (2) the explicit field vacuum contribution, $U_{\rm mag}(\sigma, B) = -P^{\rm mag}$, where $P^{\rm mag}$ was defined in (14) with $M = g\sigma$ as was done in Ref. [20]. This will be the chiral model II. In this case we have for the potential

$$U(\sigma, \vec{\pi}, B) = \frac{\lambda^2}{4}\left(\sigma^2 + \vec{\pi}^2 - f_\pi^2\right)^2 + U_{\rm mag}(\sigma, B) - U(\sigma_0, 0, B), \quad (22)$$

where

$$U_{\rm mag}(\sigma, B) = \sum_{f=u,d}\frac{N_c(|q_f|B)^2}{2\pi^2} \times \left[\zeta'(-1, x_f) - \frac{1}{2}\left(x_f^2 - x_f\right)\ln x_f + \frac{x_f^2}{4}\right], \quad (23)$$

with $x_f = (g\sigma)^2/(2|q_f|B)$ as in (14), and σ_0 is the σ field in the vacuum. The last term in (22) insures that the pressure goes to zero at zero density. Replacing this expression for the potential in the gap equation, we get

$$\sum_{f=u,d}\frac{N_c|q_f|B}{2\pi^2}\sum_\nu^{\nu_{f,\max}}\alpha_\nu\int_0^{p_{F,f\nu}}\frac{dp_z}{\sqrt{p_z^2 + m^2 + 2\nu|q_f|B}} + \frac{\lambda^2}{gm}\left(\sigma^2 - f_\pi^2\right)\sigma - \frac{|q_f|BN_c}{2\pi^2}\left[\ln\Gamma(x_f) - \frac{1}{2}\ln(2\pi) + x_f - \frac{1}{2}(2x_f - 1)\ln(x_f)\right] = 0. \quad (24)$$

In Fig. 1 we compare the quark masses in isospin-symmetric quark matter as a function of the baryon density obtained with both models and using the two approaches described above to take into account the B-dependent vacuum corrections. By construction the curves for the NJL and the chiral model I start at the same mass at zero density and decrease with density, reaching the value of the current mass of the quarks in the chiral symmetric phase. For the chiral model II the quark vacuum mass also increases with B but not so strongly. As discussed in Refs. [11–13], in the NJL model, the magnetic field shifts the chiral symmetry restoration to larger densities. The same occurs with the chiral model II. We also note that within this model the chiral symmetry restoration occurs slower than in the NJL model, a feature that is already present for zero magnetic

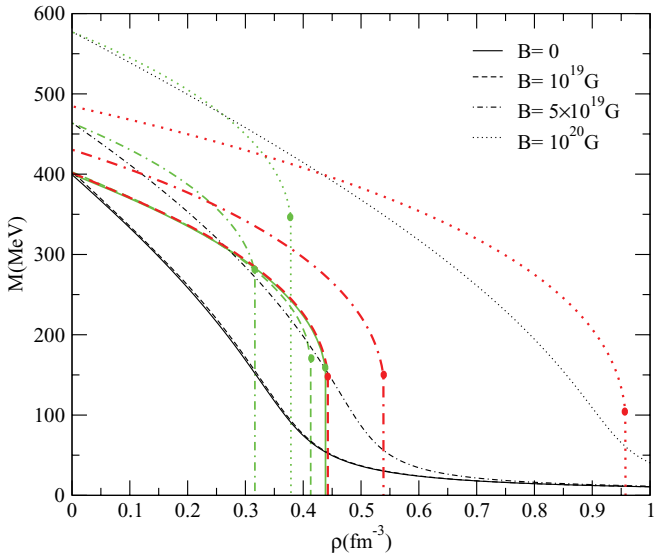

FIG. 1. (Color online) The quark mass as a function of baryon number density for isospin-symmetric quark matter, and for several values of the magnetic field. The lines correspond to the su(2) NJL (thin/black lines), the chiral model I with a renormalized f_π (medium-thick/green lines) and the chiral model II with B dependent vacuum corrections defined in (23) (thick/red lines).

field. In the chiral model I magnetic catalysis is not so clear. There are two competing effects which can be identified from the gap equation: For a larger f_π, i.e., larger vacuum quark mass, the restoration of chiral symmetry occurs at smaller densities if no Landau quantization is present in the quark quasiparticle (QP) energy. This is the effect that is observed for the smaller magnetic fields. However, Landau quantization reduces the QP energy, and, therefore, for very strong fields, the chiral symmetry restoration occurs at larger densities when B increases.

III. RESULTS

The main objective of the present section is to compare the different quark models and to discuss how the vacuum corrections due to the presence of a strong magnetic field may be taken into account in the MIT bag model and in the chiral model. We will first compare the properties of symmetric baryonic matter and, in a Sec. III B, we will discuss the implications in the EOS of stellar quark matter obtained with both chiral models considered.

A. Symmetric quark matter

In Fig. 2 the energy per baryon calculated with the chiral model, NJL model, and MIT bag model is shown for several values of the magnetic field. In the absence of an external magnetic field, the three models give similar results at high densities, when a chiral symmetry restored state is the ground state of the system. Since both the chiral model and the NJL model use low-density meson properties to fix the parameters of the models, they behave in a similar way. Below $B = 10^{19}$ G the magnetic field has no noticeable effect on the energy per particle. However, above $B = 10^{19}$ G, the effect becomes stronger and the MIT gives the lowest energy per particle. This is due to the fact that the bag pressure, which describes the vacuum effects, was kept constant, independent of the magnetic field, and, due to the Landau quantization, the contribution of the kinetic energy is strongly reduced. The minimum of the energy per particle is shifted to higher densities but not so strongly as in the other models. In the chiral model I we see that (a) in the chiral symmetry broken phase, the chiral model has a behavior similar to the NJL for large values of B, and at zero density the energy per particle of both models always coincide, and (b) although B-dependent vacuum corrections are partially taken into account and the energy per particle does not decrease so much as in the MIT bag model, in the chiral restored phase the energy per particle

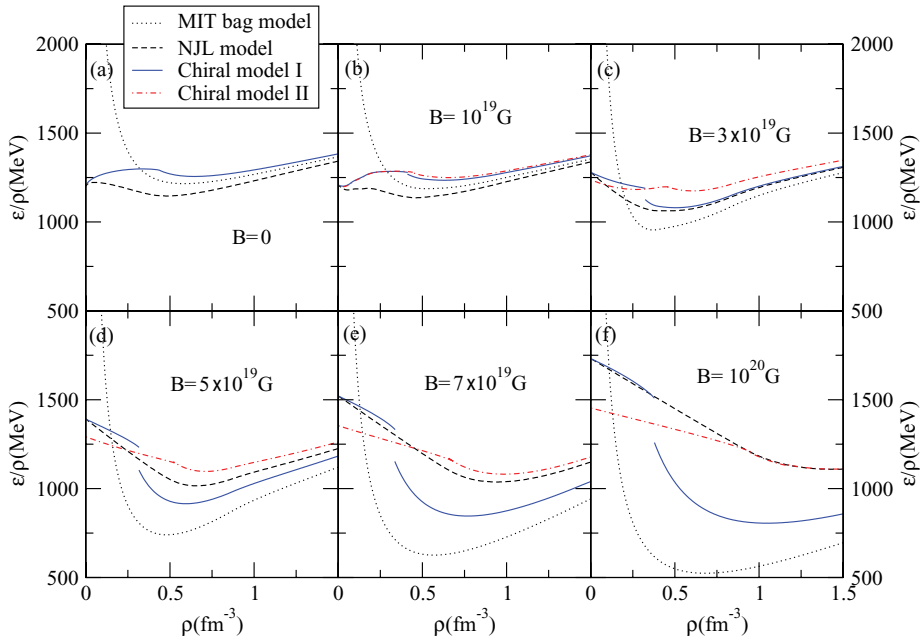

FIG. 2. (Color online) Quark matter energy per baryon number as a function of the baryon number density for isospin-symmetric quark matter, and for several values of the magnetic field. The different lines correspond to the NJL (dashed lines), chiral model I (full lines), chiral model II (dashed-dotted lines), and MIT bag model (dotted lines).

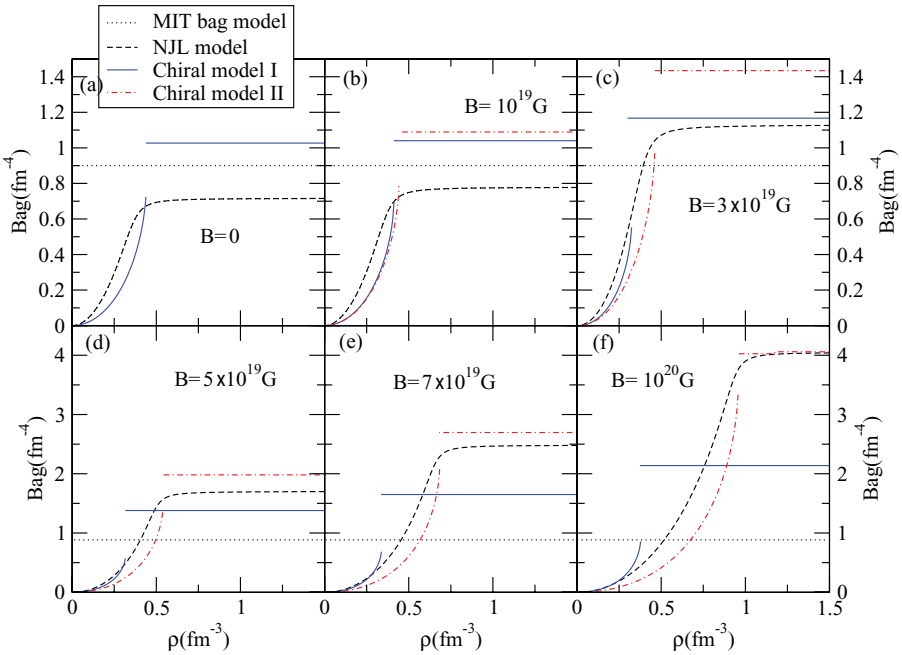

FIG. 3. (Color online) The bag pressure as a function of baryon number density for isospin-symmetric quark matter. The different lines correspond to the NJL (dashed lines), chiral model I (full lines), chiral model II (dashed-dotted lines), and MIT bag model (dotted lines). Please notice that the y-axis scale of the bottom figures is different from the one of the top figures.

is still much smaller than the predictions of both the NJL and the chiral model with the vacuum correction (23) for $B > 5 \times 10^{19}$ G. In chiral model II, where the B-dependent vacuum corrections are properly taken into account in the chiral model we conclude the following: (a) In the chiral symmetry broken phase, the chiral model predicts for $B < 3 \times 10^{19}$ G a larger energy per particle than NJL. However, for larger values of B the opposite occurs because the vacuum mass in this model does not increase so much with B than in the NJL model. (b) In the chiral restored phase the energy per particle is larger in the chiral model until a very large magnetic field (10^{20} G).

Let us define, in all models, an effective bag pressure which corresponds to the total energy minus the kinetic energy contribution. In Fig. 3 we plot the effective bag pressure for the three quark models, and several magnetic-field intensities. We have considered both approaches to the B-dependent vacuum corrections in the chiral model. For $B = 0$, all models are supposed to describe the same physics at high densities, which corresponds to the chiral restored phase: The NJL has the smallest bag pressure while the chiral model has the largest one. For the MIT, as discussed before, we have chosen an intermediate value. For finite values of B, we conclude the following: (a) In the chiral symmetry broken phase the chiral model II has the smallest effective bag pressure, although close to the one of the NJL model. The chiral model I gets closer to the NJL model as B increases, however, the chiral symmetry restoration occurs at too low densities compared with the other two chiral models. (b) In the chiral symmetry restored phase the effective bag increases with B in all models except in the MIT bag model. Within the NJL, the effective bag increases faster with B than in the chiral model II, and at $B = 10^{20}$ G both models coincide. In the chiral model I the effective bag increases too slowly and above 4×10^{19} G it is already smaller than the one obtained in the NJL model. However, we should point out that the large differences occur only for very intense magnetic fields, above 5×10^{19} G.

The behavior of the bag pressure in the different models reflects itself on the pressure of the system. In Fig. 4 we plot the pressure of the gas of symmetric quark matter as a function of density for different magnetic field intensities. Below 10^{19} G all models give results in the chiral restored phase similar to the ones obtained at $B = 0$: The model with the smallest effective bag pressure (the NJL model) has the largest pressure. Above 3×10^{19} G the different effective bag pressures of the three models give rise to quite different pressures at high densities, with the MIT bag model predicting the largest one and the chiral model II the smallest one.

B. Stellar quark matter

In a quark star, we must impose both β-equilibrium and charge neutrality. The relations between the chemical potentials of different particles are given by

$$\mu_d = \mu_u + \mu_e, \quad \mu_e = \mu_\mu. \tag{25}$$

In terms of the neutron and the electron chemical potentials μ_n and μ_e, one has

$$\mu_u = \tfrac{1}{3}\mu_n - \tfrac{2}{3}\mu_e, \quad \mu_d = \tfrac{1}{3}\mu_n + \tfrac{1}{3}\mu_e. \tag{26}$$

For the charge neutrality we impose

$$\rho_e + \rho_\mu = \tfrac{1}{3}(2\rho_u - \rho_d). \tag{27}$$

In Fig. 5, we plot the pressure and the particle fraction as a function of the baryon density obtained with the chiral model and the NJL model for different values of the magnetic-field intensity. For the chiral model, we will only consider the B-dependent vacuum effects through the renormalization of the pion decay constant, chiral model I. Since we will not go beyond $B = 10^{19}$, G both prescriptions introduced in Sec. II D give similar results.

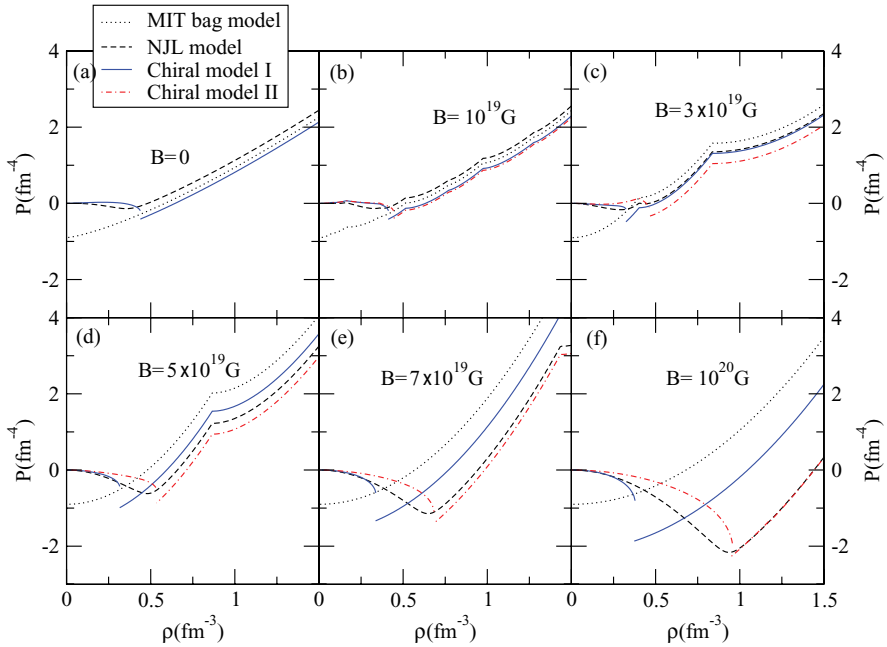

FIG. 4. (Color online) Pressure as a function of baryon number density for isospin-symmetric quark matter, and for several values of the magnetic field. The different lines correspond to the NJL (dashed lines), chiral model I (full lines), chiral model II (dashed-dotted lines), and MIT bag model (dotted lines).

At the surface of the quark star, defined by a zero pressure, the density is finite. The chiral model predicts larger baryon densities at the surface and a softer EOS for magnetic fields below 10^{19} G. For larger fields the opposite occurs, e.g., NJL predicts larger densities at the surface. However, according to the scalar virial theorem [26], the interior magnetic field strength could be as large as $B \sim 1$–3×10^{18} G so, in principle, fields stronger than the ones represented in Fig. 5 will not occur in the interior of compact stars.

Considering the particle fractions obtained within both models, it is seen that the NJL model predicts a larger u-quark fraction, and consequently larger electron and muon fractions. At $B = 10^{19}$ G the main effects due to the magnetic field occur below $\rho = 0.25$ fm^{-3}. The irregularity of the curves is due to the filling of the LLs, which may give rise to strong fluctuations on the particle fractions. There is a large increase of the u quark, and correspondingly of the electron fraction, with the increase of B. It is even observed that the u-quark fraction is larger than the d-quark fraction in a small range of densities. However, we should point out that, according to the pressure plots, the density at the surface of the star will be above 0.5 fm^{-3}. Therefore, the strong effects on the particle fractions below that density will not affect the star properties, except if the star has a crust as discussed in Refs. [27] and [28]. In this case strong effects could occur in the star crust. The onset of the muon is sensitive to the field and reflects the filling of the lepton LLs; larger muon fractions are attained at high density due to the larger u-quark fractions. For the chiral model the muon fraction is always below 0.001 in the absence of a magnetic field. This changes for a magnetic field stronger

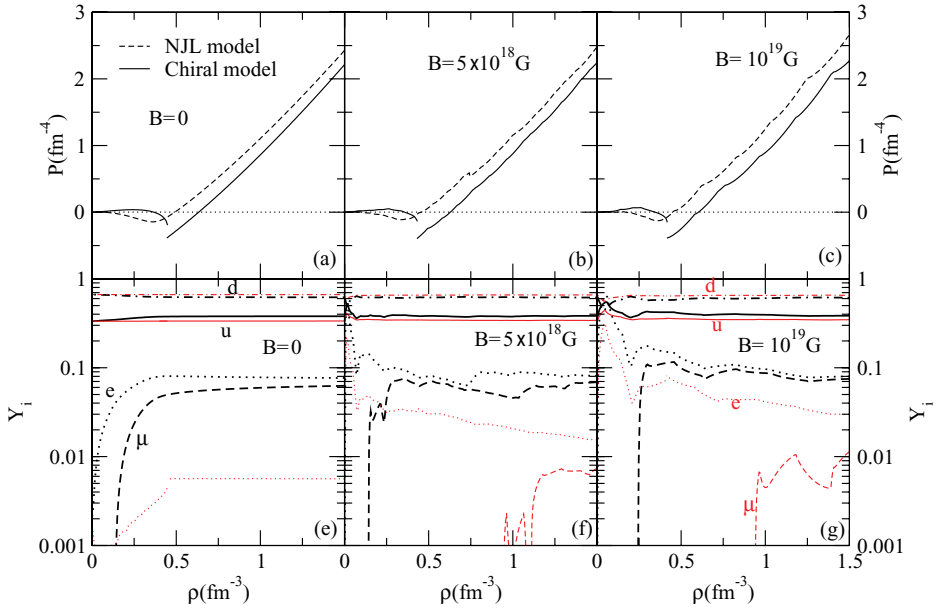

FIG. 5. (Color online) Pressure (top) and particle fractions (bottom) as a function of baryon number density for asymmetric quark matter, and for $B = 0$, 5×10^{18}, 10^{19} G. The thin line is for the su(2) NJL model and the thick line is for the chiral model. The zero axis is shown in the pressure plots with a thin dotted line. In the bottom plots the black (thick) lines are for the su(2) NJL model and the red (thin) lines for the chiral model I.

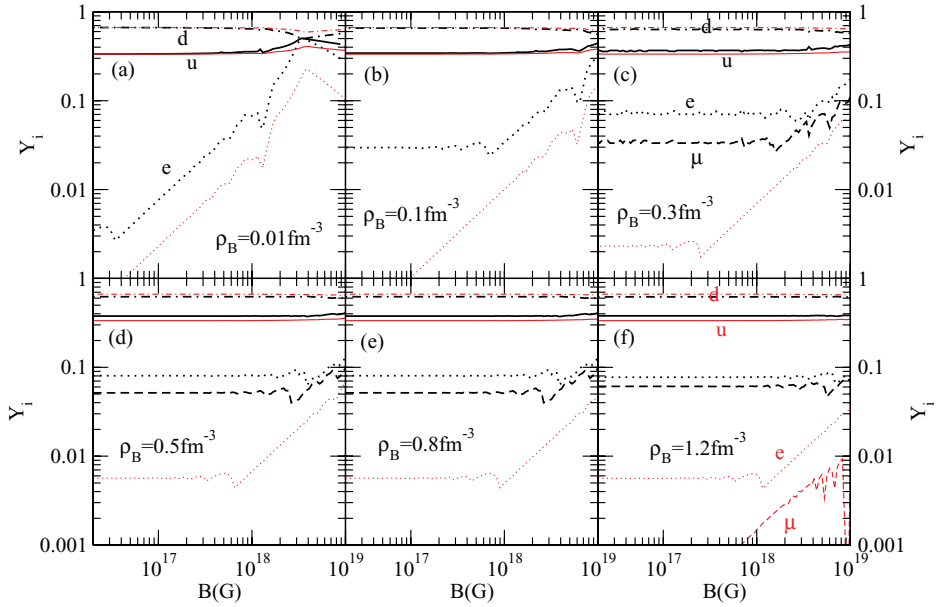

FIG. 6. (Color online) Quark and lepton fractions as a function of the magnetic field for asymmetric quark matter, and for several values of the baryonic density ($\rho = 0.001$, 0.01, 0.3, 0.5, 0.8, 1.2 fm^{-3}). The black (thick) lines are for the su(2) NJL model and red (thin) lines for the chiral model.

than 10^{18} G for densities above 1 fm^{-3} as seen in Figs. 5 and 6.

In order to better understand the effect of the magnetic field on the particle fractions we plot in Fig. 6 the particle fractions as a function of the magnetic-field intensity for six representative densities: The densities below 0.3 fm^{-3} would only occur in the crust of the star, in the case it exists, ∼0.5 fm^{-3} is the surface density, and 0.8 and 1.2 fm^{-3} are baryon densities in the interior of the star. At the surface the electron and muon fractions are larger for the NJL model. This has implications in the possible existence of a crust [27]. A larger electron fraction will be able to support a larger crust. In Ref. [29] it was shown that NJL would predict a larger electron fraction at the surface than the MIT bag model. The chiral model seems to behave more as the MIT bag model. At the surface of a star with no crust, the effect of the magnetic field starts to be non-negligible for $B > 7 \times 10^{17}$ G, with a clear increase of the electron fraction in the chiral model. This effect will occur for much smaller fields in a star with a crust, as can be seen in Fig. 6(a). As a result, it is expected that the structure of the crust will be deeply influenced by the presence of a very strong magnetic field.

The effect of the magnetic field on the muon fraction within the chiral model is also clearly seen in this figure: For $\rho =$ 1.2 fm^{-3} the muon fractions rises above 0.001 for fields a bit below 10^{18} G.

IV. CONCLUSIONS

In the present work we have compared the properties of quark matter under a strong magnetic field described using three different models: the MIT bag model [8], which describes quark matter in a chiral restored phase, the chiral model [17,18], and the two-flavor NJL model [10], both described by a chiral symmetric Lagrangian density. We have discussed the effect of the magnetic field on the vacuum properties and how the parameters of the models related to the vacuum should be chosen in order to take into account vacuum corrections. However, these corrections are only important for very strong magnetic fields $B > 3 \times 10^{19}$ G, which are not expected to be found in compact stars but could be formed as short-lived magnetic fields in relativistic heavy-ion collisions playing an important role in possible experimental signatures of strong charge parity (CP) violation and the phenomenon of the chiral magnetic effect [30]. Estimations done in Ref. [31] show that for the large hadron collider (LHC) energy it could be possible to get $eB \sim 15m_\pi^2$, which corresponds to a field $B \sim 5 \times 10^{19}$ G.

It was shown that if the schematic MIT quark model is used to describe quark matter under strong magnetic fields, the value of the bag pressure should be adjusted in order to account for the magnetic-field vacuum corrections. In the chiral model the vacuum corrections may be taken into account by fitting the parameters of the model to a quark vacuum mass that includes these corrections, chiral model I, or by including B-dependent vacuum corrections as discussed in Ref. [20], chiral model II. It was shown that for very strong fields, above 5×10^{19} G, the chiral model I failed to include adequately the B-dependent vacuum correction. However, below those extreme magnetic fields, chiral model I gave reasonable results. Although chiral model II behaves as the NJL model, there are some important differences: Its vacuum mass does not increase as fast as the one of the NJL when B increases. As a result, in the chiral model II the energy per particle in the chiral symmetric broken phase becomes smaller than the one of NJL for very large B values. In the chiral symmetric phase the effective bag pressure increases faster with B in the NJL model. Therefore, although the bag pressure is smaller in the NJL for $B = 0$, at $B = 10^{20}$ G, NJL and the chiral model II have the same bag pressure.

Finally, we have applied the chiral model and the two-flavor NJL model to the description of stellar matter. It was shown that, within the chiral model, quark stars will have a larger baryon density at the surface. This feature could be reversed for a strong magnetic field larger than 3×10^{19}. However, such strong magnetic fields are not expected to exist in compact stars. Another difference is the larger (smaller) u (d) quark fractions in the NJL model. As a consequence, the chiral model predicts much smaller lepton fractions. One of the main effects of the magnetic field is to increase the u-quark fractions at low densities due to their larger absolute charges, and, therefore, also the electron fractions. This could have strong effects on the structure of the crust of a quark star as the one predicted in Ref. [28].

ACKNOWLEDGMENTS

We thank João da Providência for valuable discussions. A.R. specially acknowledges helpful discussions with Prafulla K. Panda at the beginning of this work. This work was partially supported by FEDER and FCT (Portugal) under the projects CERN/FP/109316/2009 and PTDC/FIS/113292/2009, and by Compstar, an ESF Research Networking Programme.

[1] R. C. Duncan and C. Thompson, Astrophys. J. **392**, L9 (1992).
[2] V. V. Usov, Nature (London) **357**, 472 (1992).
[3] B. Paczyński, Acta Astronomica **42**, 145 (1992).
[4] McGill SGR/AXP Online Catalog, [http://www.physics.mcgill.ca/∼pulsar/magnetar/main.html].
[5] N. Itoh, Prog. Theor. Phys. **44**, 291 (1970); A. R. Bodmer, Phys. Rev. D **4**, 1601 (1971); E. Witten, *ibid*. **30**, 272 (1984).
[6] Z. Berezhiani, I. Bombaci, A. Drago, F. Frontera, and A. Lavagno, Astrophys. J. **586**, 1250 (2003); I. Bombaci, I. Parenti, and I. Vidana, *ibid*. **614**, 314 (2004); I. Bombaci, P. K. Panda, C. Providencia, and I. Vidana, Phys. Rev. D **77**, 083002 (2008).
[7] S. Chakrabarty, Phys. Rev. D **54**, 1306 (1996).
[8] A. Chodos, R. L. Jaffe, K. Johnson, C. B. Thorne, and V. F. Weisskopf, Phys. Rev. D **9**, 3471 (1974).
[9] R. G. Felipe, A. P. Martínez, H. P. Rojas, and M. Orsaria, Phys. Rev. C **77**, 015807 (2008).
[10] Y. Nambu and G. Jona-Lasinio, Phys. Rev. **122**, 345 (1961); **124**, 246 (1961).
[11] D. Ebert and K. G. Klimenko, Nucl. Phys. A **728**, 203 (2003).
[12] D. P. Menezes, M. B. Pinto, S. S. Avancini, A. P. Martínez, and C. Providência, Phys. Rev. C **79**, 035807 (2009).
[13] D. P. Menezes, M. Benghi Pinto, S. S. Avancini, and C. Providência, Phys. Rev. C **80**, 065805 (2009).
[14] S. P. Klevansky and R. H. Lemmer, Phys. Rev. D **39**, 3478 (1989); V. P. Gusynin, V. A. Miransky, and I. A. Shovkovy, Phys. Lett. B **349**, 477 (1995); Nucl. Phys. B **462**, 249 (1996).
[15] E. S. Fraga and A. J. Mizher, Phys. Rev. D **78**, 025016 (2008).
[16] M. Gell-Mann and M. Levy, Nuovo Cimento **16**, 705 (1960).
[17] M. C. Birse and M. K. Banerjee, Phys. Lett. B **136**, 284 (1984); S. Kahana, G. Ripka, and V. Soni, Nucl. Phys. A **415**, 351 (1984).
[18] M. Kutschera, W. Broniowski, and A. Kotlorz, Nucl. Phys. A **516**, 566 (1990).
[19] Koichi Takahashi, J. Phys. G **32**, 1131 (2006); **34**, 653 (2007).
[20] Ana Júlia Mizher, M. N. Chernodub, and Eduardo S. Fraga, Phys. Rev. D **82**, 105016 (2010).
[21] R. Gatto and M. Ruggieri, Phys. Rev. D **82**, 054027 (2010); **83**, 034016 (2011).
[22] M. D'Elia, S. Mukherjee, and F. Sanfilippo, Phys. Rev. D **82**, 051501 (2010).
[23] V. Soni and D. Bhattacharya, Phys. Rev. D **69**, 074001 (2004).
[24] A. Rabhi, H. Pais, P. K. Panda, and C. Providência, J. Phys. G **36**, 115204 (2009).
[25] M. Buballa, Nucl. Phys. A **611**, 393 (1996); Phys. Rep. **407**, 205 (2005).
[26] D. Lai and S. Shapiro, Astrophys. J. **383**, 745 (1991).
[27] Ch. Kettner, F. Weber, M. K. Weigel, and N. K. Glendenning, Phys. Rev. D **51**, 1440 (1995).
[28] Prashanth Jaikumar, Sanjay Reddy, and Andrew W. Steiner, Phys. Rev. Lett. **96**, 041101 (2006).
[29] D. P. Menezes, C. Providência, and D. B. Melrose, J. Phys. G **32**, 1081 (2006).
[30] I. V. Selyuzhenkov (STAR Collaboration), Rom. Rep. Phys. **58**, 049 (2006); D. E. Kharzeev, Phys. Lett. B **633**, 260 (2006); D. E. Kharzeev, L. D. MacLerran, and H. J. Waringa, Nucl. Phys. A **803**, 227 (2008).
[31] V. Skokov, A. Illarionov, and V. Toneev, Int. J. Mod. Phys. A **24**, 5925 (2009).